Reverse *I-V* and *C-V* characteristics of Schottky barrier type diodes on Zn doped InP epilayers grown by metalorganic vapor phase epitaxy

A. Singh and P. Cova
Universidad de Oriente, Departamento de Física, Laboratorio de Semiconductores, Apartado 188, Cumaná 6101, Sucre, Venezuela

R. A. Masut
Groupe de Recherche en Physique et Technologie des Couches Minces, Département de Génie Physique, École Polytechnique, C.P. 6079, Succ. Centre-Ville, Montréal, Québec H3C 3A7, Canada

(Received 15 November 1993; accepted for publication 2 May 1994)

Mesa etched, Au/p-InP Schottky diodes with a thin interface layer [metal-thin interface layer-semiconductor (MIS) diodes] were fabricated by evaporation of Au onto a Zn doped epitaxial layer of InP grown by low pressure metalorganic vapor phase epitaxy, on a highly doped InP substrate. The reverse current-voltage (I_r-V_r) and 1 MHz capacitance-voltage (C-V) characteristics of the Au/p-InP MIS diodes were measured in the temperature range 220–393 K. The reverse current in the MIS diodes did not saturate but increased with the increase in the reverse bias voltage. The soft I_r-V_r characteristics of the epitaxial Au/p-InP MIS diodes were very well described by the interface layer thermionic emission theory of Wu [J. Appl. Phys. **51**, 3786 (1980)] for reverse bias voltages in the range 0–5 V and over the temperature range 300–393 K. In this temperature range, the values of the zero bias barrier height (ϕ_{b0}) obtained from the analysis of the I_r-V_r/T characteristic using the self-consistent iterative least square fitting method of Tseng and Wu [J. Appl. Phys. **61**, 299 (1987)] agreed very well with those obtained from the C-V/T data. The analysis of the I_r-V_r/T data provided the values of $(7.5\pm1.7)\times10^{-3}$ and (45±22) Å for the transmission coefficient and the thickness of the interface layer, respectively. The capacitance-frequency (C-f) data for frequencies in the range 1 kHz up to 1 MHz and for bias voltages between −0.2 and 4.0 V, justify the assumption of voltage independence of the charge trapped in the states localized at the interface layer, made in the analysis of both the I_r-V_r/T and C-V/T data.

I. INTRODUCTION

InP is a promising material for the manufacture of solar cells for space applications, high speed field-effect transistors (FETs), optoelectronic, and microwave devices. Fabrication of good quality metal-semiconductor (MS) and metal-thin interface layer-semiconductor (MIS) junctions is vital to the efficient operation of InP-based devices such as high speed FETs and MIS solar cells. Much effort has been devoted to the study of MS and MIS junctions to bulk p-type semiconductor[1–11] and only a few reports are found on the junctions based on epitaxial p-InP layers grown by metalorganic vapor phase epitaxy (MOVPE).[12] However, to the best of our knowledge, a detailed study of the reverse characteristics in MIS contacts to bulk or epitaxial p-type InP has not been conducted.

From a technological point of view, the Schottky barrier height is the most important device parameter because it controls both, the current-voltage (I-V) and the capacitance-voltage (C-V) characteristics in MS and MIS diodes. To obtain the correct value of the Schottky barrier height from the I-V data, it is imperative to establish the current transport mechanisms prior to the calculation of the barrier height. To identify the mechanisms of current transport, I-V measurements at different temperatures are needed. Hokelek and Robinson[1,2] studied the Schottky contacts of various metals on chemically etched surfaces of p-type InP substrate. They deduced the values of the Schottky barrier height from the room temperature reverse-biased C-V and forward-biased I-V characteristics using standard techniques[1] valid for ideal Schottky diodes. To determine the barrier height from the I-V data, they assumed that under forward bias, thermionic emission (TE) was the dominant mechanism of current transport and used the theoretical value of 60 A cm^{-2} K^{-2} for the effective Richardson constant (A^*) for p-type InP. However, their values of Schottky barrier heights to p-type InP, obtained by the C-V technique did not agree with those determined by the I-V method.[2]

During the process of fabrication of Schottky contacts to a chemically etched semiconductor surface, an interface layer between the metal and semiconductor is unavoidably formed which introduces non-ideality in the forward I-V characteristics due to the bias dependence of the barrier height. Moreover, the majority carriers have to tunnel through the barrier presented by the interface layer which results in the reduction of current in a manner equivalent to a reduction in the effective Richardson constant. The I-V characteristics of a Schottky diode with interface layer can be described by the interface layer-thermionic emission (ITE) theory of Wu[13] which incorporates the effects of the applied voltage and transmission coefficient across the interface layer in the thermionic emission theory.

We fabricated Au/p-InP epitaxial Schottky barrier type diodes by electron beam evaporation of Au on a chemically etched surface of p-InP epilayers grown by MOVPE. The room temperature forward I-V characteristics of these diodes were nonideal with an ideality factor of 1.18. This fact indicated that pure thermionic emission was not responsible for

 0021-8979/94/76(4)/2336/7/$6.00 © 1994 American Institute of Physics

current transport, and the standard techniques of barrier height determination used by Hokelek and Robinson[1] could not be employed in our case. We have followed a more realistic approach to determine the characteristic diode parameters (barrier height, effective Richardson constant, etc.) from the simultaneous analysis of the reverse current-voltage/temperature (I_r-V_r/T) and 1 MHz capacitance-voltage/temperature (C-V/T) data.

We report a new method to determine the characteristic parameters of the Schottky diodes with interface layer, which makes use simultaneously of both I_r-V_r/T and high frequency C-V/T data. Since the measured soft behavior of I_r-V_r characteristics of the Au/p-InP epitaxial diodes suggested the existence of a thin interface layer between Au and the p-InP epilayer, we fitted the I_r-V_r/T data with Wu's theoretical expression for reverse current,[13] using the self-consistent iterative least square fitting method of Tseng and Wu.[14] This fitting procedure provided the values of the zero bias barrier height and the ratio of the interface layer thickness to its dielectric constant. Using this value of the ratio of the layer thickness to its dielectric constant, the high frequency C-V data at different temperatures were fitted to the C^{-2} vs V relation including the effects of interface layer,[15] and the values of the zero bias barrier height and carrier concentration at that temperature were determined. The effective Richardson constant was used as an adjustable parameter to obtain good agreement between the values of zero bias barrier height obtained from the I_r-V_r and C-V data. The assumption of voltage independence of the charge trapped in the states at the interface layer, made in the analysis of both the I_r-V_r/T and the high frequency C-V/T data, was justified by the capacitance-frequency (C-f) measurements at different bias voltages.

The theoretical background and experimental techniques are presented in Secs. II and III, respectively. The experimental results are analyzed in Sec. IV. In Sec. V, the results are discussed and a summary is presented.

II. THEORETICAL BACKGROUND

The C-V characteristics of metal-interface layer-semiconductor (MIS) diodes have been theoretically investigated by various authors.[15–18] For a MIS diode in which the bias dependence of charge at the interface states is negligible, the C^{-2} vs V relation can be written as[15]

$$C^{-2}=2(V_0+V)/q\epsilon_s A^2(N_A-N_D), \tag{1}$$

where V is the applied voltage. For a p-type semiconductor, V is positive for the reverse bias and negative for the forward bias, ϵ_s is the semiconductor permittivity, N_A-N_D is the net acceptor concentration in the p-type semiconductor and A the area of the rectifying contact. V_0, the intercept of C^{-2} with the voltage axis, is related to the zero bias barrier height (ϕ_{b0}) through the equation[15]

$$\phi_{b0}=\{V_0^{1/2}-(\delta/\epsilon_i)[q\epsilon_s(N_A-N_D)/2]^{1/2}\}^2+V_p+kT/q \tag{2}$$

with

$$V_p=(kT/q)\ln[N_V/(N_A-N_D)], \tag{3}$$

where ϵ_i is the permittivity and δ the thickness of the interface layer. N_V is the effective density of states in the valence band. The net acceptor density (N_A-N_D) is still determined from the slope of the C^{-2} vs V curve using[15]

$$N_A-N_D=2/[q\epsilon_s A^2(dC^{-2}/dV)]. \tag{4}$$

The interface layer-thermionic emission (ITE) theory of Wu[13] for the majority carrier current transport across a MIS diode predicts that the reverse current-voltage (I_r-V_r) characteristics under nonequilibrium conditions for a p-type semiconductor are given by[13]

$$I_r=AA_{\rm eff}T^2\exp(-q\phi_{br}/kT)[1-\exp(-qV_r/kT)] \tag{5}$$

with

$$A_{\rm eff}=A^*\Theta_p \tag{6}$$

and

$$A^*=4\pi qm^*k^2/h^3, \tag{7}$$

$$\Theta_p=\exp[-2\delta(2m^*\chi)^{1/2}/\hbar], \tag{8}$$

where I_r is the reverse current, V_r the applied reverse voltage, A^* the effective Richardson constant ($A^*=60$ A cm^{-2} K^{-2} for p-type InP[19]), Θ_p the transmission coefficient of the holes across the interface layer, m^* the effective tunneling mass of holes, χ the effective barrier height presented by the interfacial layer, and ϕ_{br} is the effective barrier height under reverse bias condition.

From Eq. (5), when the reverse bias, $V_r>3kT/q$, the reverse current I_r can be expressed as

$$I_r=AA_{\rm eff}T^2\exp(-q\phi_{br}/kT). \tag{9}$$

In this formulation, ϕ_{br} depends on the applied reverse voltage through the image force barrier lowering ($\Delta\phi_b$) and the voltage drop across the interface layer (V_i) and is given by

$$\phi_{br}=\phi_{b0}-\Delta\phi_b-V_i, \tag{10}$$

where ϕ_{b0} is the zero bias barrier height without image force lowering. The image force lowering of the barrier height $\Delta\phi_b$ arises from the electrostatic attraction between an electron and its image in the metal and is given by[20]

$$\Delta\phi_b=[q^3(N_A-N_D)(\phi_{b0}-V_p-kT/q+V_s)/8\pi^2\epsilon_s^3]^{1/4}. \tag{11}$$

Assuming that the net charge trapped in the interface states remains constant under most of the applied reverse bias voltages, V_i under reverse bias may be expressed as

$$V_i=\Delta Q_{\rm sc}/C_i=[Q_{\rm sc}(V_s)-Q_{\rm sc}(0)]/C_i, \tag{12}$$

and Eq. (10) for ϕ_{br} becomes

$$\phi_{br}+\Delta\phi_b=\phi_{b0}-\Delta Q_{\rm sc}/C_i, \tag{13}$$

where $C_i=\epsilon_i/\delta$ is the capacitance per unit area of the interface layer, and $Q_{\rm sc}(V_s)$ is the space charge density in the surface depletion layer of the semiconductor under nonequilibrium which is a function of the applied voltage drop across the semiconductor, and in the depletion approximation, can be written as[21]

$$Q_{\rm sc}(V_s)=[2q\epsilon_s(N_A-N_D)(\phi_{b0}-V_p-kT/q+V_s)]^{1/2}, \tag{14}$$

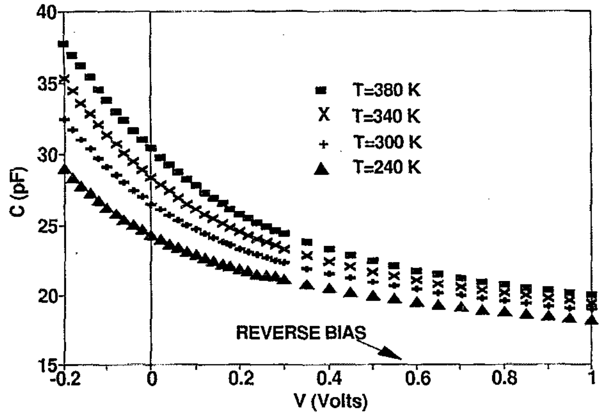

FIG. 1. Capacitance-voltage data for an epitaxial Au/p-InP MIS junction, at 1 MHz with temperature as a parameter.

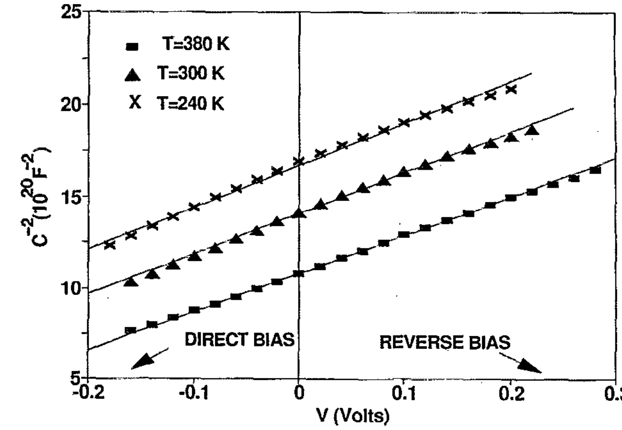

FIG. 2. Temperature variation of C^{-2} vs V characteristics at 1 MHz for the Au-MIS diode on epitaxial p-InP layer.

where $V_s = V_r - V_i$ is the applied voltage drop across the semiconductor. Both V_s and V_i are positive quantities for the p-type semiconductor under reverse bias.

III. EXPERIMENTAL METHOD

The epitaxial InP layer used in this work is approximately 2.5 μm thick, grown by low pressure MOVPE on a highly doped p-type InP substrate. The precursors were trimethylindium (TMIn) and phosphine (PH_3) with a V/III ratio of 250. The layer was doped during growth using diethyl zinc (DEZn). Before ohmic contact deposition, the samples were degreased with electronic grade trichloroethylene, acetone, and propanol at 40 °C for 10 min and then chemically etched with $1HF{:}1HCl{:}1H_2O_2{:}4H_2O$. Ohmic contact to the InP substrate was obtained by thermal evaporation of Au/Zn/Au at a pressure of about 1×10^{-6} Torr and annealing for 6 min at 375 °C in $N_2{:}H_2$ (90:10) gas. Schottky contacts to the epitaxial p-type InP layer were fabricated by electron beam evaporation of Au at a pressure of about 5×10^{-7} Torr. Rectangular Schottky contacts with area 4.76×10^{-4} cm^2 were defined by standard photolithography and lift off techniques and mesa etched with $3(1M\ K_2Cr_3O_7){:}1H_2SO_4{:}2HCl$ at 60 °C for 7 min.

The reverse current-voltage characteristics of the epitaxial Au/p-InP MIS diodes were measured using two 619 Keithley electrometers and a Keithley 230 programmable power supply. The small signal ac capacitance (C_m) and parallel conductance (G_m) as a function of applied voltage (V), in the frequency range between 1 kHz up to 1 MHz, were simultaneously measured with a Hewlett–Packard 4192A LF impedance analyzer.

The epitaxial Au/p-InP MIS diodes were mounted in a liquid nitrogen cryostat and the I_r-V_r, 1 MHz C_m-V and G_m-V measurements were carried out over the temperature range 220–393 K. The C-f measurements were carried out at 300 and 393 K. The sample temperature was controlled by a Lakeshore DRC-84C temperature controller.

IV. EXPERIMENTAL DATA AND ANALYSIS

A. C-V/T and C-f/V data for a Au/p-InP epitaxial MIS diode

For the Au/p-InP epitaxial MIS diodes, the 1 MHz C_m and G_m were measured as a function of bias voltages at different temperatures between 220 and 393 K. The junction capacitance C was obtained from C_m by means of a procedure described in detail elsewhere.[22] A set of C vs V plots are shown in Fig. 1 and some typical C^{-2} vs V curves are shown in Fig. 2. For bias voltages between -0.2 and 0.3 V, the curves show linearity over the entire temperature range of our experiments. The experimental values of C^{-2} shown in Fig. 2 (discrete points) fit well to Eq. (1) (Fig. 2, solid lines), and the values of V_0 and $N_A - N_D$ obtained from the least square fitting procedure are listed in Table I.

The frequency variation of the room temperature junction capacitance C for the Au/p-InP MIS diode at different bias voltages is shown in Fig. 3.

TABLE I. Summary of the electrical parameters for the Au/p-InP epitaxial Schottky diode with interface layer, determined from the C-V/T and reverse I-V/T data. The uncertainties in barrier height determined from the I_r-V_r and C-V data are approximately 5 and 20 mV, respectively.

T (K)	$N_A - N_D$ (10^{16} cm^{-3})	V_0 (mV)	ϕ_{b0} (mV) from C-V	ϕ_{b0} (mV) from I-V
393	2.4	510	761	757
380	2.4	513	754	756
362	2.4	539	762	761
340	2.3	565	763	766
320	2.3	598	771	773
300	2.3	632	775	769
272	2.2	685	783	761
261	2.2	701	779	758
240	2.2	733	788	725
220	1.9	780	826	681

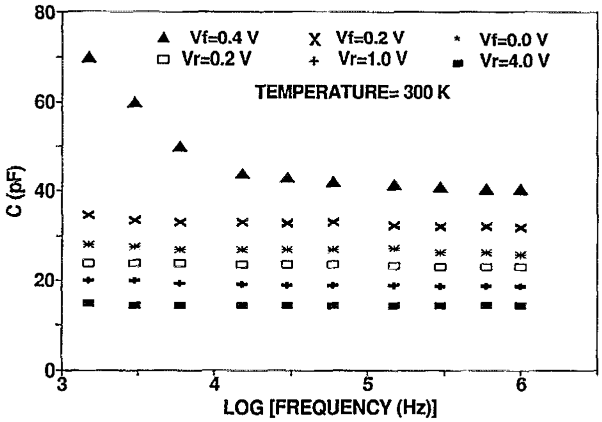

FIG. 3. Capacitance-frequency characteristics of the epitaxial Au/p-InP MIS diode with bias voltage as a parameter.

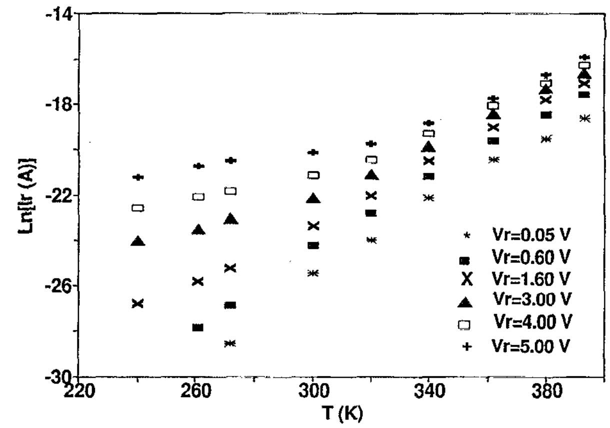

FIG. 5. Reverse current-temperature characteristics of the epitaxial Au/p-InP MIS diode with reverse bias voltage as a parameter.

B. Reverse *I*-*V*/*T* and *I*-*T*/*V* data for the Au/*p*-InP MIS diode

The reverse current-voltage (I_r-V_r) and current-temperature (I_r-T) characteristics were measured in the temperature range 220–393 K for reverse bias voltages between 0 and 5 V. A set of I_r-V_r/T and I_r-T/V_r characteristics are shown in Figs. 4 and 5, respectively.

Some typical ln (I_r/T^2) vs $1/T$ plots are shown in Fig. 6. It is clear from Fig. 6 that for low reverse bias voltage (V_r=0.2 V), ln (I_r/T^2) vs $1/T$ is linear over the temperature range 261–393 K. However, the length of the linear segment shrinks with the increase in the reverse bias voltage, and for V_r=5.0 V, the linearity is obeyed only at temperatures above 300 K. The effective Schottky barrier height (ϕ_{br}) is calculated from the gradient of the lines in Fig. 6 from the following relation:

$$\phi_{br} = -(k/q)d[\ln(I_r/T^2)]/d(1/T). \tag{15}$$

The reverse bias voltage dependence of ϕ_{br} is shown in Fig. 7.

The experimental values of the reverse current $I_r(V_r)$ at T=380 K, shown in Fig. 4 (+ signs) were analyzed in terms of the ITE model [Eq. (5)] to determine the characteristic parameters ($\phi_{b0}, A_{\text{eff}}$, and C_i) of the MIS diode. The reverse bias dependence of the effective Schottky barrier height ϕ_{br} was calculated from the equation

$$\phi_{br} = -(kT/q)\ln\{I_r(V_r)/(AA_{\text{eff}}T^2) \times[1-\exp(-qV_r/kT)]\}. \tag{16}$$

Substituting in Eq. (16), $A=4.76\times10^{-4}$ cm^2, the experimental values of $I_r(V_r)$ at T=380 K from Fig. 4, and using some initial value for A_{eff}, the reverse bias voltage dependence of ϕ_{br} was calculated. Using the value of N_A-N_D for T=380 K given in Table I, replacing V_s by V_r and inputting an initial value for ϕ_{b0}, $\Delta\phi_b$, and ΔQ_{sc} were calculated as a function of V_r, from Eqs. (11) and (14), respectively. Following the self-consistent iteration method described by Tseng and Wu,[14] both ϕ_{b0} and C_i were determined by least square fitting the values of $\phi_{br}+\Delta\phi_b$ to Eq. (13). The iterative process converged after three iterations. Substituting in Eq. (2), the value of $1/C_i=\delta/\epsilon_i$ obtained from the above fitting procedure and using the values of V_0 and N_A-N_D at T=380 K from Table I, the value of ϕ_{b0} for the C-V data was estimated. Since the values of ϕ_{b0} at T=380 K obtained from the I_r-V_r and C-V data were not in good agree-

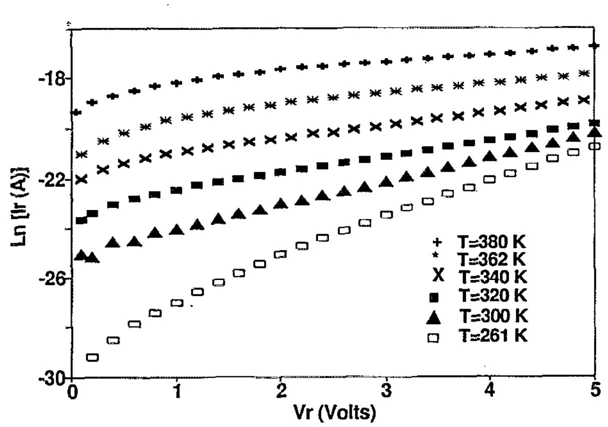

FIG. 4. Reverse current-voltage data at different temperatures for a Au-MIS diode on epitaxial p-InP layer.

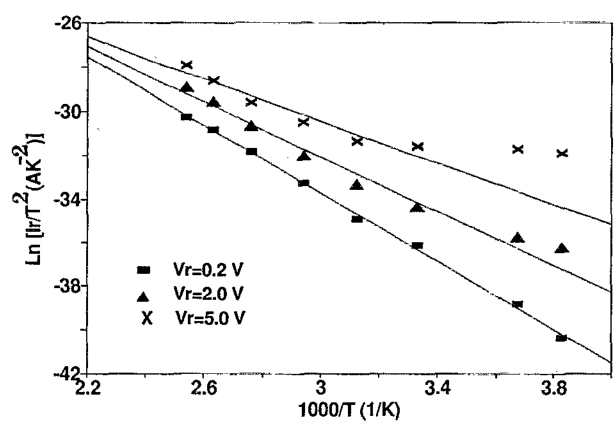

FIG. 6. ln $[I_r/T^2]$ vs $1000/T$ plots at different reverse bias voltages for the epitaxial Au/p-InP MIS diode.

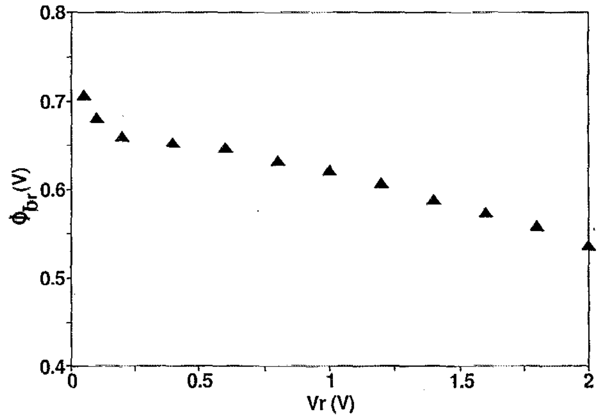

FIG. 7. Reverse voltage dependence of the effective barrier height of the MIS diode shown in Fig. 6.

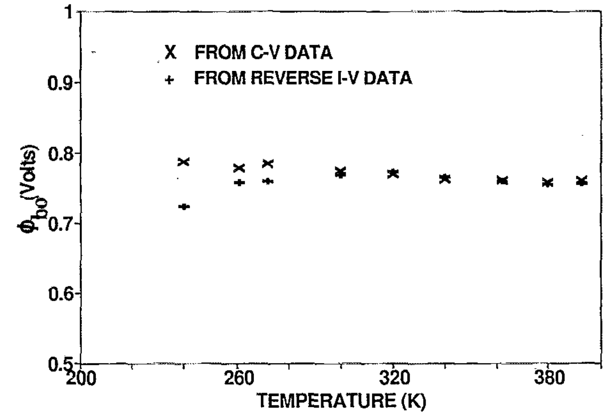

FIG. 9. Temperature variation of the zero bias barrier height for the epitaxial Au/p-InP MIS diode, obtained from the I_r-V_r/T and C-V/T data.

ment, the value of A_{eff} was adjusted and the self-consistent iterative least square fitting procedure explained above was repeated. Finally, a good agreement between the values of ϕ_{b0} calculated from the I_r-V_r and C-V data at $T=380$ K was obtained with

$$A_{\mathrm{eff}}=(0.45\pm0.10)\ \mathrm{A\,K^{-2}\,cm^{-2}},$$

$$\phi_{b0}=(0.755\pm0.005)\ \mathrm{V}, \tag{17}$$

$$C_i=(3.00\pm0.06)\ \mu\mathrm{F/cm^2}.$$

The experimental values of ln $\{I_r/[1-\exp(-qV_r/kT)]\}$ at $T=380$ K (Fig. 8, $\times$ signs) gave a very good fit to Eq. (5) (Fig. 8, solid line) over the entire range of reverse bias voltages used in our experiments.

In the analysis of the rest of the I_r-V_r/T data shown in Fig. 4, a fixed value of $A_{\mathrm{eff}}=0.45$ A K^{-2} cm^{-2} from Eq. (17) was substituted in Eq. (16) to transform the experimental I_r-V_r values (Fig. 4) into ϕ_{br} vs V_r, and the self-consistent iterative fitting procedure explained above was repeated to determine the values of ϕ_{b0} and C_i at different temperatures. The values of C_i thus obtained, along with the corresponding values of V_0 and N_A-N_D listed in Table I, were substituted

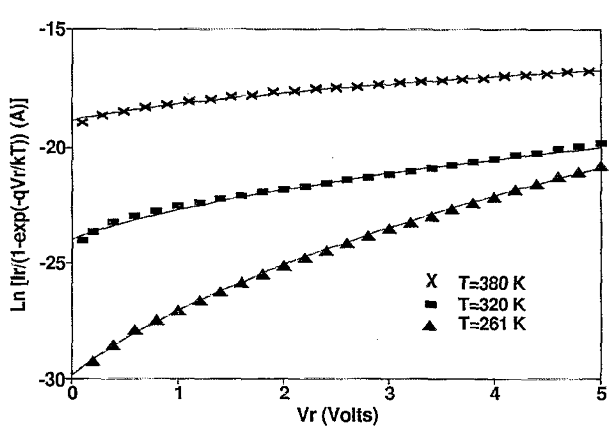

FIG. 8. ln $\{I_r/[1-\exp(-qV_r/kT)]\}$ vs V_r plots for the epitaxial Au/p-InP MIS diode. The solid lines are the best fit of the experimental values at different temperatures (discrete points) to the theoretical Eq. (5).

in Eq. (2) to determine $\phi_{b0}(T)$ from the C-V data. The values of ϕ_{b0} obtained from both the reverse I-V and C-V data are given in Table I and are plotted as function of temperature in Fig. 9.

V. DISCUSSION

The measured reverse current in the Au/p-InP MIS diode shown in Fig. 4, increases with an increase in the reverse bias voltage. Among a number of processes which can cause the "soft" reverse current-voltage characteristics, a common one is tunneling. The parameter E_{00} which plays an important role in the tunneling theory of Pandovani and Stratton[23] and Crowell and Rideout[24] can be expressed as

$$E_{00}=1.85\times10^{-11}[(N_A-N_D)/m_rK_s]^{1/2}, \tag{18}$$

where $m_r=m^*/m_0$ is the ratio of the effective mass to the free electron mass ($m_r=0.5$ for p-type InP[19]), K_s is the dielectric constant of the semiconductor ($K_s=12.35$ for InP[25]) and N_A-N_D is the effective hole concentration expressed in cm^{-3}. The ratio kT/E_{00} determines the relative importance of thermionic emission and tunneling. The dominant process of current transport should be field emission (FE) if $kT/qE_{00}\ll1$, thermionic field emission (TFE) if $kT/qE_{00}\approx1$ and thermionic emission (TE) if $kT/qE_{00}\gg1$. Substituting in Eq. (18) the values of N_A-N_D from Table I, and using $m_r=0.5$ and $K_s=12.35$, $E_{00}=1.15$ mV was estimated. For temperatures in the range 240–393 K, the ratio kT/E_{00} is between 18 and 29. This indicates that the Au/p-InP epitaxial MIS device operates in a region where the TE current transport mechanism is predominant. Therefore, the contribution of tunneling to the soft reverse I-V characteristics of the epitaxial Au/p-InP can be safely ruled out.

For reverse bias voltages in the range 0–5 V, the calculated values of the ratio of the diffusion velocity to the thermal velocity are between 20 and 60. This also suggests that in our work, the current transport is explained by the thermionic emission theory of Bethe[26] rather than by the diffusion theory of Schottky.[27]

The linearity of the measured ln $[I_r/T^2]$ vs $1/T$ characteristics for the epitaxial Au/p-InP MIS diodes shown in Fig.

6 provided direct experimental evidence in favor of thermionic emission as the dominant mechanism of current transport at least over the temperature range 300–393 K for the entire range of reverse bias voltages used in our experiments. For $V_r<1.4$ V, thermionic emission is the current limiting process for temperatures between 261 and 393 K. The effective barrier height obtained from the experimental data shown in Fig. 6, shows a gradual decrease with the increase in the reverse bias voltage (Fig. 7). Thus, the soft reverse current in the Au/p-InP epitaxial diode shown in Fig. 4 may be explained by using a bias dependent barrier height in the thermionic emission theory.

The inclusion of image force lowering of the barrier height in the TE theory results in a $(V_r)^{1/4}$ dependence of the effective barrier height ϕ_{br} and of the logarithm of the reverse current. However, the image force effect alone was not enough to account for the observed bias dependence of the reverse current (Fig. 4) and the Schottky barrier height (Fig. 7).

The interface layer between the metal and semiconductor, unavoidably formed during the process of device fabrication, also gives rise to bias dependent Schottky barrier height and results in soft reverse I-V characteristics. Therefore, we analyzed the reverse I-V characteristics of the Au/p-InP epitaxial Schottky barrier type contacts in terms of the interface layer thermionic emission (ITE) model of Wu,[13] which incorporates the effects of the applied voltage drop and transmission coefficient across the interface layer and image force effects into the thermionic emission theory. The voltage dependence of the reverse current measured at different temperatures (Fig. 8, discrete points) was well described in terms of the ITE model of Wu (Fig. 8, solid lines). The values of ϕ_{b0} for the Au/p-InP epitaxial MIS diode, obtained by fitting the measured reverse I_r-V_r to the ITE model [Eq. (5)] also agreed very well with those determined from the C-V data over the temperature range 300–393 K (Fig. 9). For temperatures 272 and 261 K, the small difference between the two values of ϕ_{b0} could be due to experimental errors. However, for $T\leqslant240$ K, the values of ϕ_{b0} obtained from the I-V data did not agree with those estimated from the C-V measurements (Fig. 9 and Table I). A close examination of Figs. 6 and 9, reveals that the good agreement between the values of ϕ_{b0} determined from the I-V and C-V methods occurs over the temperature range 300–393 K where thermionic emission is the dominant mechanism of current transport. Below 300 K, the deviations between the values of ϕ_{b0} obtained from the two methods (Fig. 9) seems to occur due to the departure of the I_r-V_r characteristics from the interface layer thermionic emission theory [Eq. (5)] of Wu.[13]

The value of $A_{\text{eff}}=(0.45\pm0.10)$ A K^{-2} cm^{-2} was determined from the analysis of the I_r-V_r data at a high temperature ($T=380$ K), where TE was definitely the dominant mechanism of current transport over the entire range of reverse bias voltages used in our experiments. Considering A_{eff} to be temperature independent, its value estimated from the high temperature I_r-V_r data was used in the analysis of the reverse current-voltage measurements at all other temperatures. Substituting in Eq. (6) the value of A_{eff} from Eq. (17), and using $A^*=60$ A K^{-2} cm^{-2},[16] the transmission coefficient $\Theta_p=(7.5\pm1.7)\times10^{-3}$ was calculated. Using this value of Θ_p in Eq. (8), a value of 4.9±0.3 for the tunneling factor $2\delta[2m^*\chi]^{1/2}/\hbar$ was estimated. In the temperature range 300–393 K, the average value of $C_i=(2\pm1)$ μF/cm^2, obtained by fitting the reverse I-V/T data to the ITE model [Eq. (5)], provided a value of (4.4±2.2) Å for the effective thickness (δ/K_i) of the interface layer. The dielectric constant K_i of the interface layer is not precisely known. Assuming $K_i=10.3$,[28] a value of (45±22) Å for the thickness of the interface layer is estimated.

Our analysis of both the reverse I-V and C-V characteristics of the Au/p-InP MIS diode is based on the assumption that the charge in the trapping states in the interface layer is independent of the bias voltage. For this assumption to be valid, the junction capacitance C should not show any frequency dispersion. To check this, we measured the capacitance of the Au/p-InP epitaxial MIS Schottky diode as a function of frequency for various bias voltages, at 300 and 393 K. The room temperature C-f/V measurements shown in Fig. 3, clearly indicate that C is essentially independent of the frequency, for the direct bias voltages below 0.2 V and for all the reverse voltages in the range 0–4.0 V. The C-f/V characteristics measured at $T=393$ K (not shown) also indicated a similar behavior. The independence of junction capacitance from the frequency (Fig. 3) indicates that the charge residing in the states in the interface layer was constant for the bias voltages between −0.2 and 4.0 V. Therefore, the assumption of voltage independence of the charge in the interface states made in our analysis of the I_r-V_r/T and C-V/T characteristics is fully justified.

In summary, the Au/p-InP epitaxial Schottky diodes studied in this work had a metal-interface layer-semiconductor (MIS) type structure with an interface layer of 45±22 Å. The charge trapped in the states in the interface layer was independent of the bias voltage for forward bias below 0.2 V and for all reverse bias voltages in the range 0–4 V. The reverse current in the MIS diode did not saturate but increased with the increase in the reverse bias voltage. Tunneling was not responsible for the observed soft reverse I-V characteristics and the image force lowering of the barrier height alone could also not explain the soft reverse characteristics of the diodes. The voltage dependence of the reverse current measured at different temperatures was well described by the interface layer thermionic emission (ITE) theory of Wu[13] with a transmission coefficient of $(7.5\pm1.7)\times10^{-3}$. The values of the zero bias barrier height obtained from the analysis of the measured I_r-V_r characteristics in terms of the ITE model agreed very well with those estimated from the C-V measurements over the temperature range 300–393 K. The discrepancy between the values of ϕ_{b0} obtained from the I_r-V_r and C-V data at temperatures below 300 K may be due to the failure of the interface layer thermionic emission mechanism to fully control the current transport in the epitaxial Au/p-InP junction.

ACKNOWLEDGMENTS

This work was partially supported by the Natural Science and Engineering Research Council of Canada

(NSERC), by the Fonds pour la Formation de Chercheurs et l'Aide à la Recherche (FCAR, Government of Québec), and the Consejo de Investigación de la Universidad de Oriente with Contract No. CI-05-022-00456/92.

[1] E. Hokelek and G. Y. Robinson, Solid-State Electron. **24**, 99 (1981).
[2] E. Hokelek and G. Y. Robinson, Appl. Phys. Lett. **40**, 426 (1982).
[3] Y. P. Song, R. L. Van Meirhaeghe, W. H. Laflere, and F. Cardon, Solid-State Electron. **29**, 633 (1986).
[4] L. M. O. Van Den Berghe, R. L. Van Meirhaeghe, W. M. Laflere, and F. Cardon, Solid-State Electron. **29**, 1109 (1986).
[5] F. Chekir, G. N. Lu, and C. Barret, Solid-State Electron. **29**, 519 (1986).
[6] K. C. Reinhardt, A. Singh, and W. A. Anderson, Solid-State Electron. **31**, 1537 (1988).
[7] A. Singh and W. A. Anderson, J. Appl. Phys. **64**, 3999 (1988).
[8] A. Singh and W. A. Anderson, J. Appl. Phys. **66**, 722 (1989).
[9] A. Singh, W. A. Anderson, Y. S. Lee, and K. Jiao, Proc. SPIE **1144**, 61 (1989).
[10] A. Singh, K. C. Reinhardt, and W. A. Anderson, J. Appl. Phys. **68**, 3475 (1990).
[11] A. Singh, K. C. Reinhardt, and W. A. Anderson, J. Appl. Phys. **71**, 4788 (1992).
[12] S. W. S. McKeever, R. J. Walters, S. R. Messenger, and G. P. Summers, J. Appl. Phys. **69**, 1435 (1991).
[13] C. Y. Wu, J. Appl. Phys. **51**, 3786 (1980).
[14] H. H. Tseng and C. Y. Wu, J. Appl. Phys. **61**, 299 (1987).
[15] K. Hattori, M. Yuito, and T. Amakusa, Phys. Status Solidi A **73**, 157 (1982).
[16] A. M. Goodman, J. Appl. Phys. **34**, 329 (1963).
[17] A. M. Cowley, J. Appl. Phys. **37**, 3024 (1966).
[18] S. J. Fonash, J. Appl. Phys. **54**, 1966 (1983).
[19] C. W. Wilmsen, *Physics and Chemistry of III-V Compound Semiconductor Interfaces* (Plenum, New York, 1985), p. 87.
[20] E. H. Rhoderic, *Metal-Semiconductor Contacts* (Clarendon, Oxford, 1988), p. 36.
[21] S. M. Sze, *Physics of Semiconductor Devices* (Wiley, New York, 1981), p. 248.
[22] A. Singh, Solid-State Electron. **28**, 223 (1985).
[23] F. Pandovani and R. Stratton, Solid-State Electron. **9**, 695 (1966).
[24] C. R. Crowell and V. Rideout, Solid-State Electron. **12**, 189 (1969).
[25] A. Fahrenbruch and R. H. Bube, *Photovoltaic Solar Energy Conversion* (Academic, New York, 1983), p. 42.
[26] H. A. Bethe, MIT Radiation Lab. Report 43/12 (1942).
[27] W. Schottky, Phys. Z. **32**, 833 (1931).
[28] M. Yamaguchi and K. Ando, J. Appl. Phys. **51**, 5007 (1980).